Available online at www.sciencedirect.com
SCIENCE DIRECT®
Pergamon
Cement and Concrete Research 34 (2004) 1093–1102
CEMENT AND CONCRETE RESEARCH

Implications of the structure of cementitious wastes containing Pb(II), Cd(II), As(V), and Cr(VI) on the leaching of metals

Cheryl E. Halim[a], Rose Amal[a,*], Donia Beydoun[a], Jason A. Scott[a], Gary Low[b]

[a]*Centre for Particle and Catalyst Technologies, School of Chemical Engineering and Industrial Chemistry, The University of New South Wales, Sydney, NSW 2052, Australia*

[b]*Analytical and Environmental Chemistry Section, Department of Environment and Conservation, Lidcombe, NSW 2141, Australia*

Received 18 August 2003; accepted 24 November 2003

Abstract

Cement stabilisation has been widely applied for the immobilisation of heavy metal ions before their disposal in landfills. This paper investigated the microstructure of cementitious wastes containing Pb, Cd, As, and Cr using an electron probe microanalyser and examined the implications of the microstructure on the leaching of the metal ions. From the microstructure analysis, it was proposed that Pb, As, and Cr ions were homogeneously dispersed in the calcium silicate hydrate (C-S-H) matrix by adsorption or precipitation with calcium or silicate compounds present in the cement. However, Cd formed discrete $Cd(OH)_2$ precipitates believed to be contained within the cement pores or adsorbed on the C-S-H matrix. The leaching of metals in the pH region of 6 to 8 decreased in the following order: Cr(VI)>Cd(II)>Pb(II)>As(V). This leaching trend was found to be influenced by the manner in which the metal ions were incorporated into the cement matrix.

Keywords: Cement; Microstructure; Backscattered electron imaging; Calcium-Silicate-Hydrate (C-S-H); Leaching

1. Introduction

Solidification/stabilisation (S/S) techniques have been widely used to immobilise contaminated wastes before their disposal into the environment. Cement stabilisation is one of the most popular stabilisation techniques due to its low cost and the resultant alkaline pH rendering many metal contaminants insoluble. The leaching of heavy metals from cementitious wastes has been subject to extensive investigation in the past [1–7]. However, the relationship between the incorporation of these metals into the cement matrix and their leaching is not fully understood.

Electron microscopic techniques have been previously used for the analysis of solid waste structures [8–10]. Klich et al. [9] used these techniques for evaluating metal speciation and association of metals to different mineralogical phases in metal-contaminated soils and industrial wastes stabilised with Portland cement. They examined the mineral alterations and weathering features that affect the durability of cement and metal containment of metals in aged remediated wastes. They found that the use of the electron microscope is an important tool to evaluate the prediction of the long-term fate of metal containments in solidified and stabilised wastes. Ouki and Hills [8] used a scanning electron microscopy (SEM) technique to evaluate the effect of addition of metal nitrate on cement hydration. They found that the type and the amount of metals added are important in the microstructural development of the cement. In general, metal addition resulted in a reduction in cement hydration and total porosity.

Metal containment in cement has been extensively studied [11–15], but much conjecture remains regarding metal ion incorporation into the cement matrix. For example, studies have postulated Pb to be either adsorbed onto the calcium silicate hydrate (C-S-H) matrix of cement [4,5] or precipitated as Pb silicate [11,12]. In the instance of Cd ions, Cartledge et al. [13] suggested Cd was in the form of $Cd(OH)_2$ particles, which were encapsulated, on a microscopic scale, in the C-S-H and/or $Ca(OH)_2$ matrix of cement. Conner [15] and Park [16] proposed instead that Cd formed a double compound $CdCa(OH)_4$ and, using X-ray photoelectron spectroscopy

* Corresponding author. Tel.: +61-2-938-54361; fax: +61-2-938-55966.
E-mail address: r.amal@unsw.edu.au (R. Amal).

0008-8846/$ – see front matter © 2003 Elsevier Ltd. All rights reserved.
doi:10.1016/j.cemconres.2003.11.025

(XPS), McWhinney and Cocke [17] observed the existence of Cd oxides, carbonates, and hydroxides. The inclusion of arsenic in cement is also unclear. Akhter et al. [18] found As formed a $NaCaAsO_4 \cdot 7.5H_2O$ precipitate in cement using X-ray diffraction (XRD) studies whereas Mollah et al. [19] observed the presence of insoluble $Ca_3(AsO_4)_2$ on the surfaces of hydrating cement particles. In the case of Cr(VI), Omotoso et al. [20] found that most Cr(VI) ions were precipitated as $Ca_2CrO_5 \cdot 3H_2O$ in cement. They also postulated that CrO_4^{2-} ions released by $Ca_2CrO_5 \cdot 3H_2O$ during the hydration process might either form an amorphous material not detected by powder diffraction techniques or be incorporated in the tetrahedral silicate sites in the C-S-H matrix [20].

Although the heavy metal containment in cement has been widely studied, very few studies have attempted to correlate this with the leaching behaviour of metal ions from cement [5]. This paper will investigate the manner in which the heavy metal ions (Pb(II), Cd(II), As(V), and Cr(VI)) are incorporated into the cement matrix, and correlations between the structural configurations of the cement-stabilised wastes and the leaching of the heavy metal ions will also be developed.

2. Experimental procedures

2.1. Preparation of cementitious waste

Cementitious wastes containing selected heavy metal ions were prepared by mixing ordinary Portland cement (OPC), supplied by Australian Cement, with either lead nitrate ($Pb(NO_3)_2$), cadmium nitrate tetrahydrate ($Cd(NO_3)_2 \cdot 4H_2O$), sodium arsenate ($Na_2HAsO_4 \cdot 7H_2O$), or sodium chromate (Na_2CrO_4) solutions. A cementitious waste containing a mixture of Pb and Cd was also prepared. The metal salts were dissolved in deionised water and blended with the OPC at water to cement (W/C) ratios of 0.38, 0.44, 0.38, 0.31, and 0.47 for wastes containing Pb, Cd, As, Cr, and both Pb and Cd, respectively. The mixtures were mechanically stirred for 15 min and subsequently cured for 28 days. The cured mixtures were crushed using three consecutive crushers (jaw crusher, cone crusher, and roller crusher) and passed through a 2.4-mm-mesh sieve. The compositions of the cement samples were analysed using X-ray fluorescence (XRF) and are shown in Table 1. The incorporation of the metal ions does not alter the overall composition of the cement. The higher Na concentration observed for the As and Cr samples is a result of the addition of As and Cr as $Na_2HAsO_4 \cdot 7H_2O$ and Na_2CrO_4, respectively.

Table 1
Composition of cementitious wastes containing Pb, Cd, As, and Cr as determined by X-ray fluorescence [7]

Element	Cement composition (mg/g of waste)				
	Cement containing Pb	Cement containing Cd	Cement containing Pb and Cd	Cement containing As	Cement containing Cr
Pb	23	0.0	20	0.0	0.0
Cd	0.0	13	19	0.0	0.0
As	0.0	0.0	0.0	13	0.0
Cr	0.0	0.0	0.0	0.0	20
Al	16	15	14	16	15
C	15	20	8.0	11	9.0
Ca	340	340	341	340	340
Fe	23	22	21	23	23
K	6.6	7.5	7.9	6.6	6.6
Mg	10	10	9.4	10	10
Na	4.5	2.2	3.9	13	22
Si	74	73	67	74	73
S	8.8	8.4	8.5	8.8	8.8
Th	0.9	0.9	1.3	0.9	0.9
Ti	0.6	0.6	0.8	0.6	0.6

2.2. Microstructure analysis using the Cameca SX50 microprobe

Sample pretreatment involved mounting a sample of the cementitious waste in Araldite D/HY-951 epoxy resin followed by polishing on Kent Mk 3 polishing machines. The polishing was performed sequentially on a ceramic lap using a 3-μm Engis diamond paste with lubricating oil followed by a Texmet lap using 1-μm diamond with water as a lubricant [21]. The epoxy resins containing the samples were carbon coated such that they became conductive for the microstructure analysis.

Analysis of the coated samples by the Cameca SX50 electron probe microanalyser (EPMA) was performed at an accelerating voltage of 15 kV and current of 20 nA. The Cameca SX50 used four wavelength-dispersive spectrometers and one energy-dispersive X-ray analyser for elemental detection [22]. Quantitative analyses for elements at different points across the samples were performed and backscattered electron (BSE) images were acquired. During the quantitative analysis, characteristic X-rays generated by the elements in the sample are diffracted by a suitable analysing crystal and measured in counts per second by gas proportional detectors. The crystals and lines used for each element were chosen to give the most sensitive but noninteracting reading with other elements [22]. Using BSE, Portland cement pastes appear as contrasting light and dark areas relating to the mean atomic number of the portrayed areas [8,23]. The colours in the images range between 0 and 255 (dark to brick) grey levels. A higher average atomic number results in a higher intensity of BSE signal, reflecting a brighter colour. Thus, porosity has a black appearance, C-S-H gel and portlandite are grey in colour, while residual anhydrous cement grains are bright/white in colour [8].

Stage and beam image acquisition scans were done to provide elemental concentration maps of the samples to view phases, inclusions, and grain boundaries. The results were analysed using HIMax 6.5 and Matlab. In the Results and discussion section, the values for elemental

composition obtained by EPMA were all in weight percent.

2.3. Leaching experiments

Leaching experiments were conducted in accordance with Australian Standard AS 4439.3-1997 [24]. Cementitious waste crushed to less than 2.4 mm in diameter was mixed with acetic acid solution at a liquid to solid (L/S) ratio of 20:1 and tumbled for 18 h at a speed of 30 rpm. The concentration range of the acetic acid solutions used was between 0.1 and 5.7 M. The resulting solution (leachate) was filtered through a 0.8-μm membrane filter and the pH was measured. The samples were preserved with 2% HNO_3 before metal ion analysis using an Optima 3000 inductively coupled plasma atomic emission spectrometer (ICPAES).

3. Results and discussion

3.1. The structure of cement and contaminated cement

3.1.1. Basic structure of cement

BSE images of the particles are shown in Fig. 1(a) and (b). The cement is dominated by the presence of C-S-H as shown by the light grey regions in the images. These particles contain approximately 20% Ca, 15% Si, and 40% O, giving a Ca:Si:O ratio of approximately 1.3:1:2.7. This ratio is in good agreement with the Ca:Si:O ratio of 1.4:1:2.3 in CaH_2SiO_4 (C-S-H gel).

Larger, darker grey inclusions in the cement surface (as highlighted in Fig. 1(a)) were found to contain high amounts of either Ca or Si. An elemental balance of the composition of these particles indicated the presence of $Ca(OH)_2$, $CaCO_3$ (which may have resulted from carbonation of $Ca(OH)_2$ [25]), or unhydrated SiO_2 particles. The black "cracks" throughout the C-S-H structure (seen in Fig. 1(b)) represent pores. Fig. 1(b) also indicates the presence of small, pale grey flecks scattered throughout the C-S-H matrix. These spots were found to contain elevated concentrations of Al and Fe (up to 10%) in the form of ettringite ($3CaO{\cdot}Al_2O_3{\cdot}3CaSO_4{\cdot}32H_2O$) and other hydrated calcium compounds.

3.1.2. The structure of Pb-contaminated cement

The BSE images of Pb-contaminated cement are given in Fig. 2(a) and (b). Comparison with Fig. 1(a) and (b) indicates the addition of Pb to the cement has little effect on the morphology and structure of the particles as the Pb-spiked cementitious waste is also dominated by the C-S-H matrix. Quantitative analysis found the Pb to be evenly distributed throughout the C-S-H matrix at a concentration of 4.6 ± 0.9 wt.%.

Fig. 3(a), (b), (c), and (d) give the X-ray mapping results for Ca, Si, and Pb in the cement sample as well as the concentration profiles of each of these elements along the line AB depicted in Fig. 3(c), respectively. Fig. 3(a) and (b) show Ca and Si to be distributed throughout the cement matrix with the occasional Ca-rich or Si-rich inclusion. These inclusions are attributed to the presence of $Ca(OH)_2$, $CaCO_3$, or unhydrated SiO_2. Fig. 3(c) highlights the fact that Pb is also dispersed throughout the C-S-H matrix. This point is further supported by the Pb concentration profile in Fig. 3(d). It shows the Pb to be present at all points along the line AB given in Fig. 3(c).

3.1.3. The structure of Cd-contaminated cement

The BSE images of Cd-contaminated cement shown in Fig. 4(a) and (b) indicate that the structure of Cd-contaminated cement is dominated by C-S-H. The Cd-contaminated cement is not as granular in appearance as the Pb-contaminated cement making identification of Ca- and Si-rich particles difficult. However, located throughout the cement structure are small white particles that were found to contain high amounts of Cd (at an average of 28%). The elemental balance of these particles was on average 18% Ca, 37% O, and 6% Si, with the remaining 11% consisting of other cations such as Fe and Al.

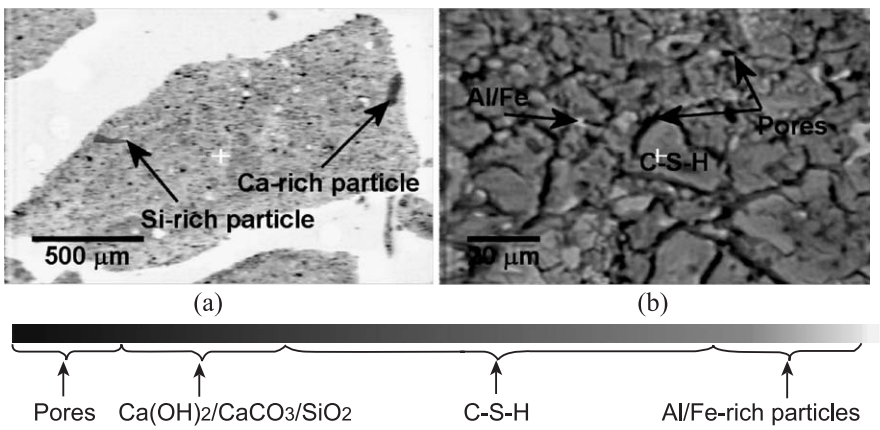

Fig. 1. BSE images of cement sample at (a) low and (b) high magnifications.

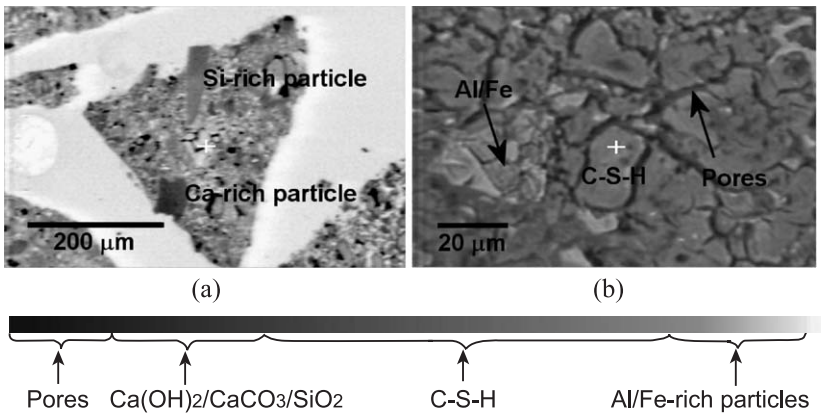

Fig. 2. BSE images of cement containing 23 mg Pb/g of waste at (a) low and (b) high magnifications.

The X-ray maps of Ca, Si, and Cd of the particle shown in Fig. 4(b) are shown in Fig. 5 as well as the concentration profiles of Cd, Ca and Si along line CD, shown in Fig. 5(c). The X-ray mapping shows Ca and Si to be distributed throughout the particle with Cd inclusions (up to 60%) at points within this matrix. Elemental analysis indicated that Cd is likely to exist as $Cd(OH)_2$ or $CdCO_3$. This is in agreement with the findings by Cartledge et al. [13] and McWhinney and Cocke [17] who reported the formation of Cd precipitates in cement as single compounds in the form of cadmium oxide, hydroxide, or carbonate [13,17]. Conner [15] and Park [16] reported Cd existed as a double cadmium calcium hydroxide compound ($CdCa(OH)_4$) [15,16].

It is clear from the images and X-ray mapping that Cd is bound differently in cement when compared to Pb. While Pb is dispersed throughout the C-S-H matrix, Cd forms discrete particles, which precipitate on the surface of C-S-H or within the cement pores.

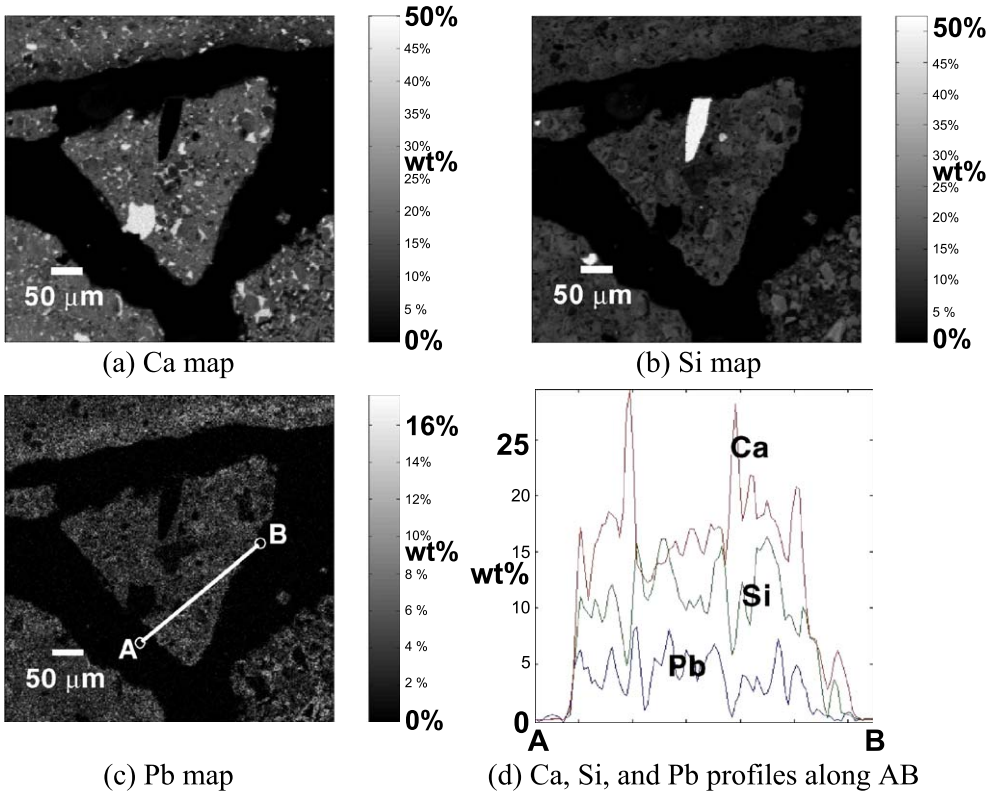

Fig. 3. X-ray maps of cement containing 23 mg Pb/g of waste. (a) Ca; (b) Si; (c) Pb; (d) Ca, Si, and Pb concentration profiles (wt.%) along line shown in (c). *X*-axis corresponds to distance along line AB.

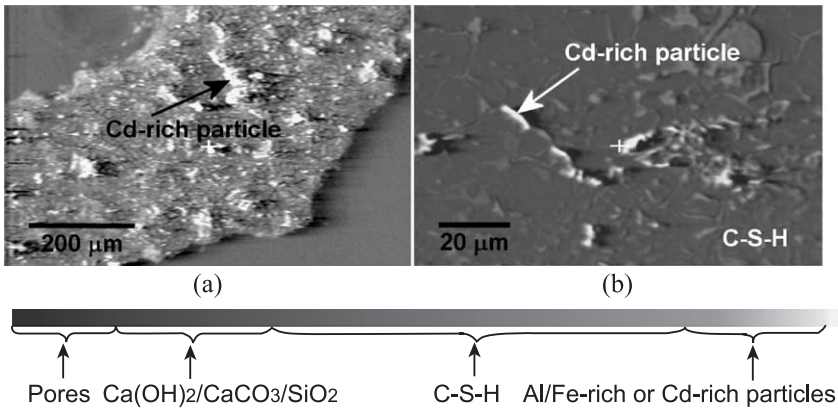

Fig. 4. BSE images of cement containing 13 mg Cd/g of waste at (a) low and (b) high magnifications.

3.1.4. The structure of cementitious waste containing both Pb and Cd

The BSE image of the cement sample is shown in Fig. 6. Fig. 7 contains the Pb and Cd X-ray maps and the concentration profiles of Pb, Cd, Ca, and Si along the line EF, shown in Fig. 7(a) and (b). From the X-ray maps, it is again apparent that Pb is distributed throughout the cement matrix, whereas Cd is concentrated (up to 30%) at various locations throughout this matrix. The results indicate that the distribution of these metals within cement is unaffected, irrespective of whether they are added individually or together.

3.1.5. The structure of As-contaminated cement

Analysis of BSE image of the As-contaminated cement (Fig. 8) indicated As to be mostly evenly distributed throughout the C-S-H matrix at a concentration of 2.5 ± 1.2%, giving an As:Ca:O ratio of 1:9.5:16. Darker areas were also observed in the image, which were found to contain high amounts of As (18 ± 3%). The As:Ca:O ratio of these

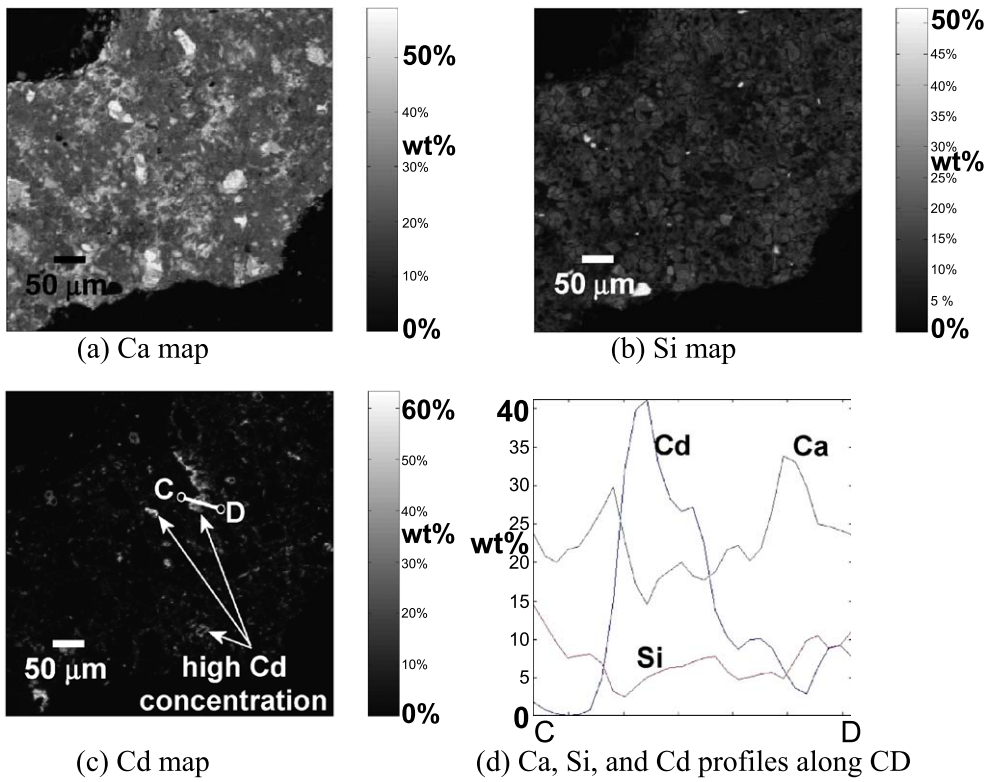

Fig. 5. X-ray maps of cement containing 13 mg Cd/g of waste. (a) Ca; (b) Si; (c) Cd; (d) Ca, Si, and Cd concentration profiles (wt.%) along line shown in (c). *X*-axis corresponds to distance along line CD.

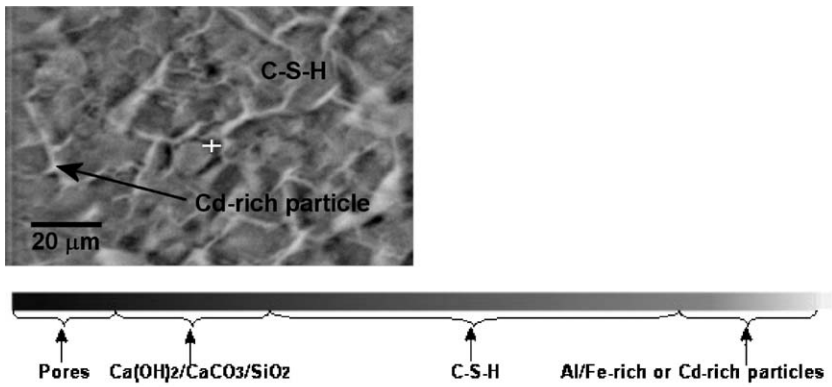

Fig. 6. BSE image of cement containing 20 mg Pb/g of waste and 13 mg Cd/g of waste.

inclusions was 1:1.7:0.5, which is comparable to the As:Ca:O ratio of $Ca_3(AsO_4)_2$ (1:0.8:0.9), suggesting that As may form a calcium arsenate precipitate. Other studies have also suggested the formation of calcium arsenate precipitates in cement, including Akhter et al. [18], who identified the $NaCaAsO_4 \cdot 7.5H_2O$ precipitate in cement, and Mollah et al. [19], who found that $Ca_3(AsO_4)_2$ precipitate was present during the hydration process.

3.1.6. The structure of Cr-contaminated cement

Fig. 9 shows the BSE image of the Cr-contaminated cement. The structure of the Cr-contaminated cement was found to be similar to that of the blank sample but with Cr evenly distributed throughout the C-S-H matrix at a concentration of 0.8 ± 0.7%. Precipitation of Cr anions with Ca in cement has also observed by Omotoso et al. [20].

3.2. Implications of metal containment in cement on leaching of metals

The leaching of heavy metal ions from cementitious wastes was studied and attempts made to link the microstructure of the cement with the extent of the observed leaching. The percentage of metal ions (Pb, Cd, As, and Cr)

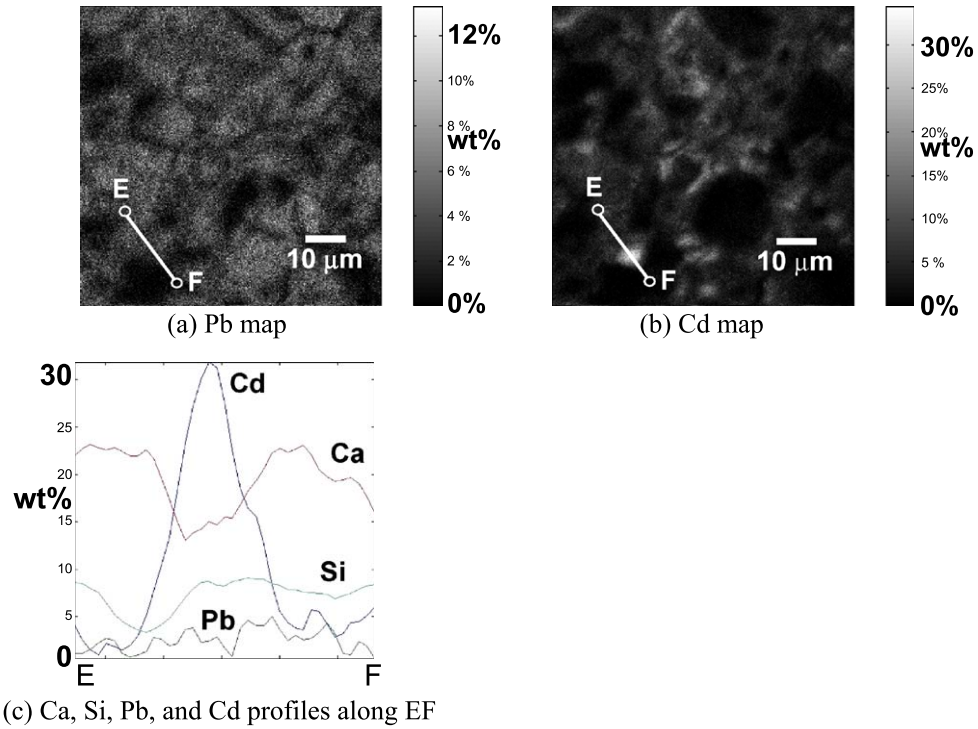

Fig. 7. X-ray maps of cement containing 20 mg Pb/g of waste and 19 mg Cd/g of waste. (a) Pb; (b) Cd; (c) Ca, Si, Pb, and Cd concentration profiles (wt.%) along line shown in (a) and (b). *X*-axis corresponds to distance along line EF.

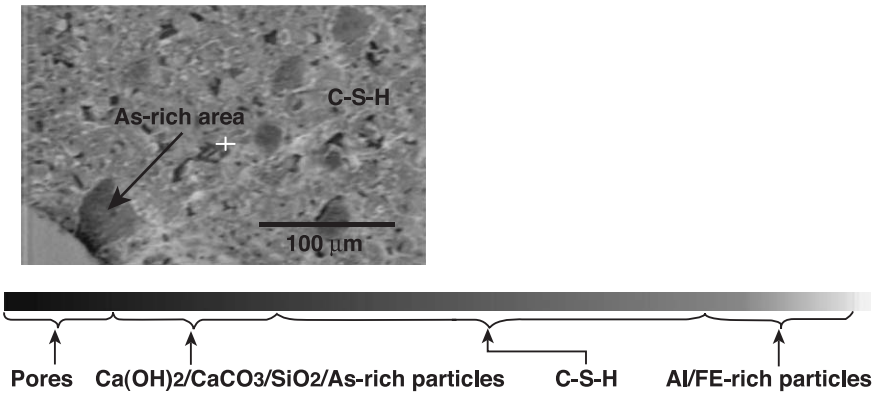

Fig. 8. BSE image of As of cement containing 13 mg As/g of waste.

leached from the cementitious waste as a function of leachate pH are illustrated in Fig. 10. It can be seen that the solubility of the heavy metal ions decreased in the following order: Cr(VI)>Cd(II)>Pb(II)>As(V) in the neutral pH region (6–8), which is the pH region typical of a mature municipal landfill leachate.

3.2.1. Calcium

In earlier studies, it has been postulated that there are two principal stages of Ca leaching from cement [26,27]. The first stage occurs when the waste is exposed to the leaching fluid and the portlandite ($Ca(OH)_2$) structure is neutralised (the region between pH 7 and 12 in Fig. 10). When the available $Ca(OH)_2$ is exhausted, the leaching fluid attacks the C-S-H matrix (the region below pH 7). This is supported by the corresponding increase of Si ions in the leachate at pH values below 7 (Fig. 11).

3.2.2. Chromium

Fig. 10 shows the relative percentage of Cr in the leachate was higher than Ca at all pH values. This shows that Cr is present as a very soluble material in cement. It is widely known that Cr(VI) is water soluble at all pH [28]. It may have formed a calcium chromate precipitate during the hydration process or adsorbed on the C-S-H matrix as chromate ions. The K_{sp} of $CaCrO_4$, a calcium chromate compound, is 7.1×10^{-4} [29], indicating the high solubility of this compound. As the Cr-contaminated cementitious waste was exposed to the leaching fluid, it is reasonable to expect that Cr would easily solubilise together with the portlandite particles.

The predicted concentration of Cr (as calcium chromate) and other ions (in mg/l) based on thermodynamic data, is shown in Fig. 12. The thermodynamic data used to provide the solubility curves in Fig. 12 were obtained from the Lawrence Livermore National Laboratory Database for PHREEQC 1.11 [30]. It was found that above pH 5, the Cr concentration in the leachate was lower than the predicted values. This is believed to be due to Cr trapped in the cement pores. Below pH 5, it can be seen that all the Cr has been completely leached as the C-S-H matrix has dissolved. This is because the C-S-H matrix has solubilised at pH 5. This assertion is supported by a corresponding increase in Si concentration in the leachate (from Fig. 11). The exact mode of Cr interaction with cement is unclear; however, studies by Fowler et al. [31] observed the formation of a water-soluble Cr precipitate in cement. They found that SiO_4^{4-} in the C-S-H matrix was substituted by CrO_4^{2-}. Omotoso et al. [20] have also reported the formation of $Ca_2CrO_5.3H_2O$ during the cement hydration process.

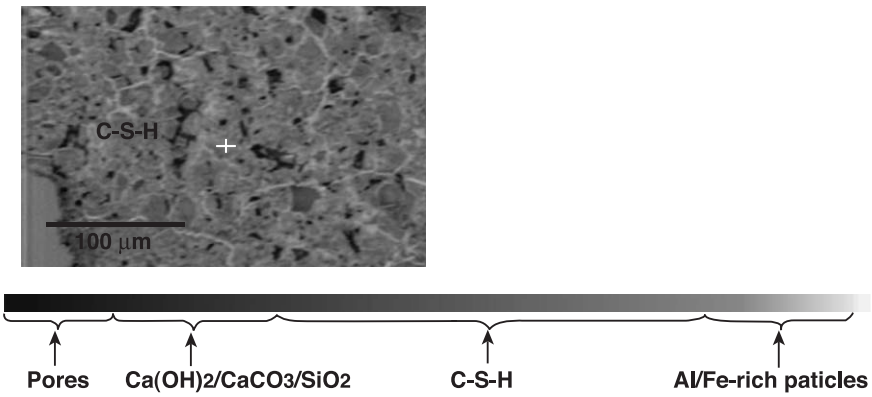

Fig. 9. BSE image of Cr of cement containing 20 mg Cr/g of waste.

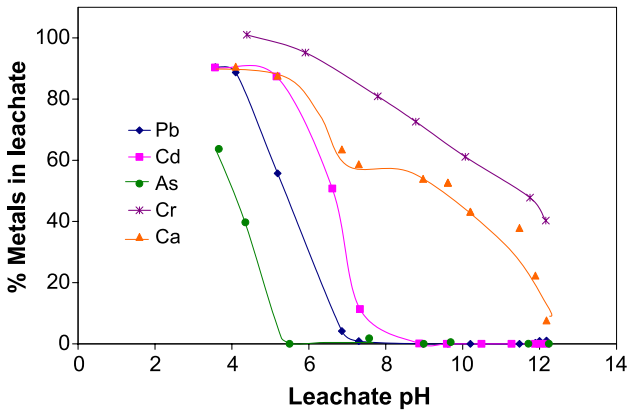

Fig. 10. Percentage of metal ions present in the leachate as a function of leachate pH. The cementitious wastes were tumbled with 0.1–5.7 M acetic acid solutions at an L/S ratio of 20:1 for 18 h. The calculation of the percentage of metal ions leached was based on the total amount of metal ions available in the wastes.

3.2.3. Cadmium

Fig. 12 shows that at pH values less than 5 the concentration of Cd in the leachate reached around 90% of the predicted value based on $Cd(OH)_2$ solubility. Earlier (in Section 3.1.3), Cd was shown to exist as discrete particles within the cement matrix that were proposed to be either cadmium hydroxide or cadmium carbonate. Upon mixing the solid waste with the leaching fluid, the $Cd(OH)_2$ particles are believed to have solubilised. Moreover, as the portlandite ($Ca(OH)_2$) was released from the cement matrix and the C-S-H solubilised, Cd trapped within the cement pores was subsequently released. This leaching mechanism is similar to that of Cr leaching; however, the presence of Cd in the leachate is also governed by the solubility of $Cd(OH)_2$. As a result, on a percentage basis, a lower amount of Cd was leached relative to Cr at a pH greater than 5 (Fig. 10). The same leaching patterns between Cd and alkalinity were also

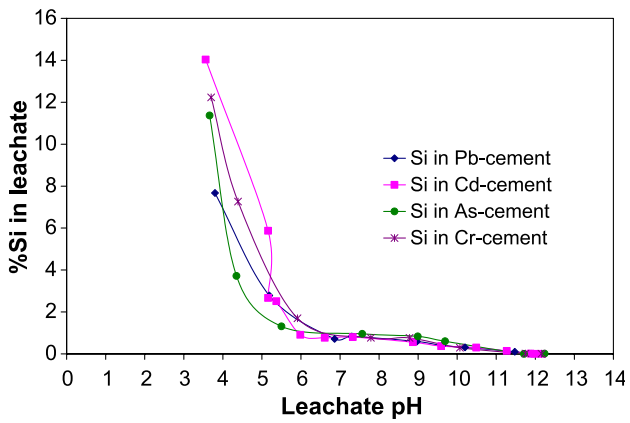

Fig. 11. Percentage of Si ions leached from Pb-, Cd-, As-, and Cr-spiked cementitious wastes as a function of leachate pH. The cementitious wastes were tumbled with 0.1–5.7 M acetic acid solutions at an L/S ratio of 20:1 for 18 h. The calculation of the percentage of Si ions leached was based on the total amount of Si ion available in the wastes.

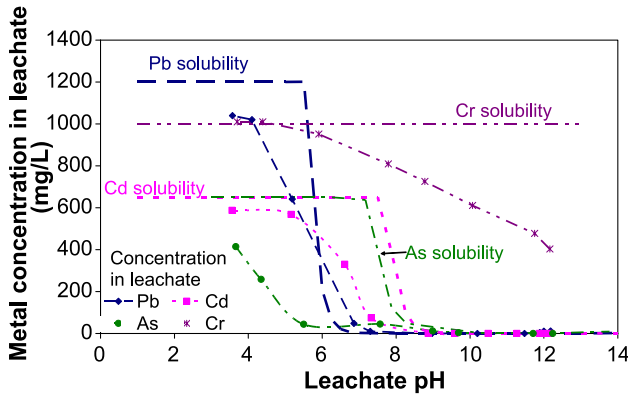

Fig. 12. Comparison of the metal concentrations in the leachate and the predicted concentrations based on the solubility of $Pb(OH)_2$, $Cd(OH)_2$, $Ca_3(AsO_4)_2$, and $CaCrO_4$.

observed by Bishop [12], supporting these findings, whereby the destruction of the C-S-H matrix releases Cd trapped within the pores (as its hydroxide or carbonate).

3.2.4. Lead

Fig. 10 shows that Pb began to rapidly leach at pH 7. At this same pH, Si also began to rapidly leach (Fig. 11). These observations indicate that Pb is primarily incorporated in the C-S-H matrix, and when this begins to dissolve and the Si is released, Pb is also released. Similar observations for Pb and Si release have been made by Bishop [12]. Fig. 11 also shows that at pH 4, the concentration of Si leached from the Pb-spiked cement was lower than that leached from the other wastes. This suggests that Pb may have formed a Pb silicate mineral in the cement, corresponding to the fact that Pb was evenly distributed in the C-S-H matrix (as shown in Section 3.1.2). The precipitation of Pb as a Pb silicate compound in cement has also been observed by Bhatty [11] and Bishop [12].

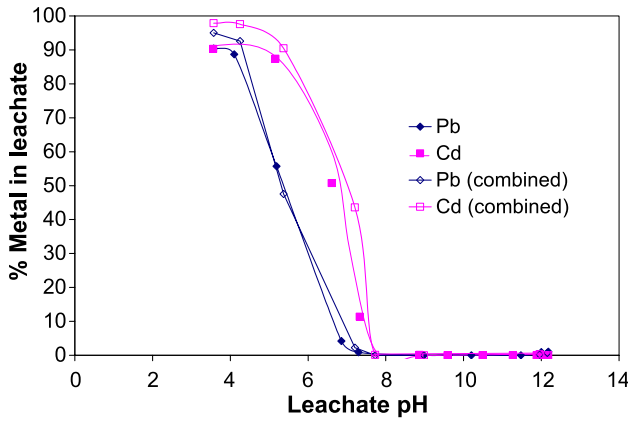

Fig. 13. Percentage of metal ions present in the leachate as a function of leachate pH for the cementitious wastes containing separate metal ions (Pb and Cd) and the cementitious waste containing both metal ions [Pb (combined) and Cd (combined)]. The calculation of the percentage of metal ions leached was based on the total amount of metal ions available in the wastes.

3.2.5. Arsenic

Similar to Pb, Fig. 10 shows that As did not completely solubilise at low pH. This shows that As is incorporated in the C-S-H matrix and forms a more complicated compound than $Ca_3(AsO_4)_2$. In addition to calcium arsenate precipitation, arsenate ion can also form iron arsenate precipitate. At this stage, however, there is not enough information to validate the proposed mechanism.

3.2.6. Lead and cadmium

The results of leaching tests carried out on the cementitious waste containing both Pb and Cd ions are presented in Fig. 13. For comparative purposes, this figure also includes the results of leaching of Pb and Cd from cement when added separately. From these tests, it is clear that the leaching of either metal is very similar whether or not the metal ions are added together or separately. This complies with the earlier imaging results that showed very little differences in the cement structure when Pb and Cd were added separately or together. This is also in agreement with findings by Neuwirth et al. [32], who observed different containment sites for Pb and Cd in cement using X-ray mapping studies. The different containment sites suggest that no interactions exist between the two elements.

4. Conclusion

From the microstructure studies of cementitious wastes, the mechanisms by which metal ions (Pb, Cd, As, and Cr) were incorporated into the cement matrix were found to differ. Pb appeared to precipitate with silicate compound in the C-S-H matrix, and As and Cr appeared to be bound into cement through adsorption or precipitation with silicates or calcium compounds in the C-S-H matrix. On the other hand, Cd formed a precipitate, present on the surface C-S-H matrix and inside the cement pores.

The manner in which the metals were incorporated into the cement matrix was found to influence the leaching mechanism. Solubility also played a role in governing the presence of the heavy metals in the leachate following release from the cement matrix. The leaching of heavy metal ions between pH 6 and 8 was found to decrease in the following order: Cr(VI)>Cd(II)>Pb(II)>As(V).

The leaching of Pb and Cd from cement was comparable irrespective of whether the metal ions were either added together or separately. This suggests that no interaction occurs between the cations when they are both added to cement.

Acknowledgements

The authors would like to thank Julie Cattle, Roy Foley, Jin Yang, Yarong Li, and Razi Uddin of the New South Wales Environmental Protection Authority for their contribution to the project. This project has been assisted by the New South Wales Government through its Environmental Trust. C.E. Halim would also like to acknowledge Rad Flossman and Barry Searle of the University of New South Wales for their assistance in polishing and electron microscopic analysis of samples.

References

[1] S.R. Hillier, C.M. Sangha, B.A. Plunkett, P.J. Walden, Long-term leaching of toxic trace metals from portland cement concrete, Cem. Concr. Res. 29 (1999) 515–521.
[2] P. Cote, Contaminant leaching from cement-based waste forms under acidic conditions, PhD Thesis, McMaster University, Hamilton, Canada, 1986.
[3] M. Hinsenveld, A shrinking core model as a fundamental representation of leaching mechanisms in cement stabilized waste, PhD Thesis, University of Cincinnati, Cincinnati, OH, 1992.
[4] K.Y. Cheng, Controlling mechanisms of metals release from cement-based waste form in acetic acid solution, PhD Thesis, University of Cincinnati, Cincinnati, OH, 1991.
[5] D.L. Cocke, The binding chemistry and leaching mechanisms of hazardous substances in cementitious solidification/stabilization systems, J. Hazard. Mater. 24 (1990) 231–253.
[6] C.E. Halim, R. Amal, D. Beydoun, J. Scott, G. Low, Leachability of lead and cadmium from cementitious waste, Proceedings of APCChE, Christchurch, 2002.
[7] C.E. Halim, R. Amal, H. Natawardaya, D. Beydoun, J. Scott, G. Low, J. Cattle, Comparison of leaching of Pb(II), Cd(II), As(V), and Cr(VI) from cementitious wastes using acetic acid and landfill leachates, Proceedings of the Eighteenth International Conference on Solid Waste Technology and Management, Philadelphia, 2003.
[8] S.K. Ouki, C.D. Hills, Microstructure of portland cement pastes containing metal nitrate salts, Waste Manage. 22 (2002) 147–151.
[9] I. Klich, L.P. Wilding, L.R. Drees, Trace metal and mineral speciation of remediated wastes using electron microscopy, Anal. Bioanal. Chem. 372 (2002) 436–443.
[10] J. Deja, Immobilization of Cr^{6+}, Cd^{2+}, Zn^{2+}, and Pb^{2+} in alkali-activated slag binders, Cem. Concr. Res. 32 (2002) 1971–1979.
[11] M.S.Y. Bhatty, Fixation of metallic ions in portland cement, Proceedings 4th National Conference on Hazardous Wastes and Hazardous Materials, Portland Cement Association, Skokie, IL, 1987, pp. 140–145.
[12] P.L. Bishop, Leaching of inorganic hazardous constituents from stabilized/solidified hazardous wastes, Hazard. Waste Hazard. Mater. 5 (2) (1988) 129–143.
[13] F.K. Cartledge, L.G. Butler, D. Chalasani, H.C. Eaton, F.P. Frey, E. Herrera, M.E. Tittlebaum, S.L. Yang, Immobilization mechanisms in solidification/stabilization of Cd and Pb salts using portland cement fixing agents, Environ. Sci. Technol. 24 (1990) 867–873.
[14] D.L. Cocke, Exploitation of the binding chemistry and leaching mechanisms to improve solidification/stabilization of hazardous wastes, Waste Manage. 13 (5–7) (1993) 520–521.
[15] J.R. Conner, Chemical Fixation and Solidification of Hazardous Wastes, Van Nostrand Reinhold, New York, 1990.
[16] C.K. Park, Hydration and solidification of hazardous wastes containing heavy metals using modified cementitious materials, Cem. Concr. Res. 30 (2000) 429–435.
[17] H.G. McWhinney, D.L. Cocke, A surface study of the chemistry of zinc, cadmium, and mercury in portland cement, Waste Manage. 13 (1993) 117–123.
[18] H. Akhter, F.K. Cartledge, A. Roy, M.E. Tittlebaum, Solidification/stabilization of arsenic salts: effects of long cure times, J. Hazard. Mater. 52 (1997) 247–264.

[19] M.Y.A. Mollah, F. Lu, D.L. Cocke, An X-ray diffraction (XRD) and Fourier transform infrared spectroscopic (FT-IR) characterization of the speciation of arsenic (V) in portland cement type-V, Sci. Total Environ. 224 (1998) 57–68.
[20] O.E. Omotoso, D.G. Ivey, R. Mikula, Hexavalent chromium in tricalcium silicate, J. Mater. Sci. 33 (1998) 507–513.
[21] R. Flossman, The preparation of thin, polished and double polished thin sections. Available from ⟨http://www.bees.unsw.edu.au/staff/general/flossman/sectioning.html⟩, last updated October 1999, accessed February 3, 2003.
[22] E.M. Unit, Cameca SX50 Microprobe. Available from ⟨http://srv.emunit.unsw.edu.au/Facilities2000_files/Equipment/_sx50.htm⟩, last updated September 13, 2002, accessed February 3, 2003.
[23] K.L. Scrivener, Microscopy methods in cement and concrete science, World Cem. Res. Dev. (1997 September) 92–112.
[24] Standards Australia, Wastes, sediments and contaminated soils: Part 3. Preparation of leachates—bottle leaching procedure, Standards Australia, Sydney, 1997.
[25] A.C. Garrabrants, F. Sanchez, D.S. Kosson, Changes in constituent equilibrium leaching and pore water characteristics of a portland cement mortar as a result of carbonation, Waste Manage. 24 (2004) 19–36.
[26] A.C. Campbell, K.M. Krupka, Application of geochemical data and modeling in performance assessments of low-level radioactive waste disposal facilities, Proceedings of Waste Management Conference, Tucson, 1997.
[27] C.E. Halim, R. Amal, D. Beydoun, J.A. Scott, G. Low, Evaluating the applicability of a modified toxicity characteristic leaching procedure (TCLP) for the classification of cementitious wastes containing lead and cadmium, J. Hazard. Mater. B103 (1–2).
[28] D.E. Kimbrough, Y. Cohen, A.M. Winer, L. Creelman, C. Mabuni, A critical assessment of chromium in the environment, Crit. Rev. Environ. Sci. Technol. 29 (1) (1999) 1–46.
[29] Selected solubility products and formation constants, at 25 °C. Available from ⟨http://chemistry.csudh.edu/oliver/chemdata/data-ksp.htm⟩, last updated 1997, accessed April 4, 2002.
[30] J. Johnson, G. Anderson, D.L. Parkhurst, Lawrence Livermore National Laboratory Database for PHREEQC 1.11, 2000.
[31] G.D. Fowler, S. Asavapisit, C.R. Cheeseman, R. Perry, A study of the chemical effects of metal hydroxides upon cement hydration reactions, in: J.M. Cases, F. Thomas (Eds.), Proceedings of International Congress on Waste Solidification–Stabilisation Processes, Societe Alpine de Publications, Nancy, France, 1995, pp. 41–45.
[32] M. Neuwirth, R. Mikula, P. Hannak, Comparative studies of metal containment in solidified matrices by scanning and transmission electron microscopy, Proceedings of The Fourth International Hazardous Waste Symposium on Environmental Aspects of Stabilization/Solidification of Hazardous and Radioactive Wastes, Atlanta, American Society for Testing and Materials, Philadelphia, PA, 1987, pp. 201–213.